Metabolic Phenotyping Reveals a Lipid Mediator Response to Ionizing Radiation

Evagelia C. Laiakis,[†] Katrin Strassburg,[‡,§] Ralf Bogumil,[∥] Steven Lai,[⊥] Rob J. Vreeken,[‡,§] Thomas Hankemeier,[‡,§] James Langridge,[⊥] Robert S. Plumb,[⊥,#] Albert J. Fornace, Jr.,[†] and Giuseppe Astarita*,[†,⊥]

[†]Department of Biochemistry and Molecular & Cellular Biology, Georgetown University, Washington DC 20057, United States
[‡]Analytical Biosciences, LACDR, Leiden University, Leiden 2333 CC, The Netherlands
[§]Netherlands Metabolomics Centre, Leiden University, Leiden 2333 CL, The Netherlands
[∥]BIOCRATES Life Sciences, Innsbruck 6020, Austria
[⊥]Health Sciences, Waters Corporation, Milford, Massachusetts 01757, United States
[#]Computational and Systems Medicine, Department of Surgery and Cancer, Faculty of Medicine, Imperial College London, London SW7 2AZ, United Kingdom

S *Supporting Information*

ABSTRACT: Exposure to ionizing radiation has dramatically increased in modern society, raising serious health concerns. The molecular response to ionizing radiation, however, is still not completely understood. Here, we screened mouse serum for metabolic alterations following an acute exposure to γ radiation using a multiplatform mass-spectrometry-based strategy. A global, molecular profiling revealed that mouse serum undergoes a series of significant molecular alterations following radiation exposure. We identified and quantified bioactive metabolites belonging to key biochemical pathways and low-abundance, oxygenated, polyunsaturated fatty acids (PUFAs) in the two groups of animals. Exposure to γ radiation induced a significant increase in the serum levels of ether phosphatidylcholines (PCs) while decreasing the levels of diacyl PCs carrying PUFAs. In exposed mice, levels of pro-inflammatory, oxygenated metabolites of arachidonic acid increased, whereas levels of anti-inflammatory metabolites of omega-3 PUFAs decreased. Our results indicate a specific serum lipidomic biosignature that could be utilized as an indicator of radiation exposure and as novel target for therapeutic intervention. Monitoring such a molecular response to radiation exposure might have implications not only for radiation pathology but also for countermeasures and personalized medicine.

KEYWORDS: *Omega-3 fatty acids, lipidomics, plasmalogens, prostaglandin, cytochrome P450*
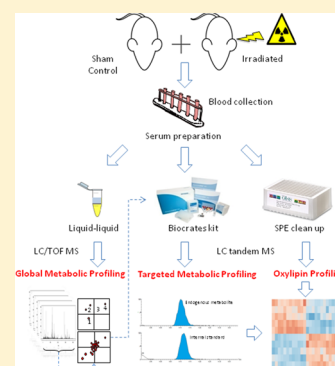
INTRODUCTION

Exposure to ionizing radiation has dramatically increased in modern society, raising serious health concerns.[1] Ionizing radiation is widely used in medicine for research, diagnosis, and therapy; it is also used in manufacturing and construction.[1−4] In addition, accidental exposure to ionizing radiation occurs during air travel and space missions. The deleterious consequences of ionizing radiation exposure can result in cancer and non-cancer-related diseases,[5,6] including cardiovascular diseases[7−13] and cognitive decline.[6] It has therefore become a priority to develop new tools that can effectively and rapidly screen populations for radiation exposures.

Methods for rapid and efficient biological dosimetry could find applications not only for estimating the risk of disease induced by medical, occupational, or accidental exposure to radiation[14] but also for countermeasures. Radiological incidents like the recent Fukushima explosion on December 2013 underscore the need for a quick and reliable way to identify exposed individuals in the days immediately following a radiological accident so that

medical management can begin as soon as possible thereafter. While cytogenetics remains the gold standard for assessing radiation exposure, such a technique might not be sensitive enough to detect subtle molecular changes evoked by radiation exposure before the occurrence of cellular and organ damage, nor does it give insight into signaling pathways triggered by ionizing radiation.

Radiation biology has traditionally focused on DNA damage and repair, mutation induction, and chromosomal rearrangements. Until recently, comparatively little attention was paid to other molecular consequences of irradiation that may underlie the risk of pathology. In addition to interacting with genomic DNA, however, ionizing radiation may alter the structure and function of key cellular components such as proteins and lipids, activating a pro-inflammatory response and ultimately affecting cell signaling.[15,16] Recent radiation research is, therefore,

beginning to adopt a systems biology approach to investigate the pleiotropic effects of exposure to ionizing radiation on multiple cellular components.[17−23]

Metabolic phenotyping is a modern analytical approach that uses state-of-the-art instrumentation such as mass spectrometry to characterize the molecular composition (i.e., the phenotype) of biofluids. To date, metabolic phenotyping investigations in radiation research have mainly focused on biomarker discovery in urine.[24−27] The capability to phenotype blood, however, provides novel opportunities to investigate the molecular response to radiation, thus yielding mechanistic insights as well as discovering novel biomarkers. Evidence indeed suggests that blood factors induced by irradiation may reflect and contribute to an ongoing inflammatory response to the initial radiation-induced injury.[28]

Here, we applied a multiplatform mass spectrometry-based metabolic phenotyping strategy to investigate in mouse serum the molecular response to acute γ-radiation exposure and describe a lipidomic biosignature that has the potential to be used as an indicator of radiation exposure and as a potential target for therapeutic interventions.

■ MATERIALS AND METHODS

Materials

All chemicals were purchased from Sigma-Aldrich (Seelze, Germany) and were of analytical-grade purity or higher. Lipid standards were purchased from Avanti Polar Lipids (Alabaster, AL, USA), Cayman Chemical (Ann Arbor, MI, USA), Biomol (Plymouth Meeting, PA, USA), and Larodan Fine Chemicals (Malmö, Sweden). For solid-phase extraction, 96-well, Waters Oasis HLB plates (60 mg) were obtained from Waters Corporation (Milford, MA, USA).

Mouse Irradiation and Sample Collection

Male C57Bl/6 mice (8−10 weeks old; $n = 5$) were irradiated at Georgetown University with 8 Gy of γ rays (^{137}Cs source, 1.67 Gy/min), corresponding to an exposure to radiation that is expected to kill half of the exposed population within 30 days ($LD_{50/30}$). Sham control male C57Bl/6 mice (8−10 weeks old; $n = 5$) were treated the same way as irradiated mice. In particular, they were transported to the irradiator at the same time, introduced into the irradiation pie, and spun in the irradiator, minus the radiation exposure. Blood was obtained by cardiac puncture 24 h following irradiation as previously reported.[14,22] Serum was collected using serum separators (BD Biosciences, CA, USA).[29] All experimental conditions and animal handling were carried out in accordance with animal protocols approved by the Georgetown University Animal Care and Use Committee (GUACUC).

Global Metabolic Profiling

Total metabolites were extracted from serum samples by 1:40 dilution in 66% acetonitrile containing 2 μM debrisoquine sulfate and 30 μM 4-nitrobenzoic acid as internal controls. Following centrifugation at 13 000g, the supernatant was stored at 80 °C for further analysis. Metabolites were separated using an ACQUITY UPLC system (Waters Corporation, Milford, MA, USA) fitted with a BEH HILIC 2.1 × 100 mm, 1.7 μm column maintained at 30 °C. The flow rate was 0.5 mL/min. Mobile phase A consisted of 95:5 acetonitrile/water (v/v) containing 10 mM ammonium acetate (pH 8.0); mobile phase B consisted of 50:50 acetonitrile/water (v/v) containing 10 mM ammonium acetate (pH 8.0). A 10 min linear gradient from 100 to 80% A with a 3 min

re-equilibration time was applied. MS analyses were performed on a Synapt G2-S mass spectrometer (Waters Corporation, Wilmslow, UK) acquiring from 50 to 1500 m/z in positive electrospray ionization mode. Capillary voltage was 2.8 kV. Data were collected in two channels all of the time: low collision energy (6.0 V), for the molecular ions, and high collision energy (15−40 V), for product ions. The ion mobility spectrometry (IMS) gas was nitrogen, and the IMS T-wave velocity and height were 900 m/s and 40 V, respectively.

Lipids were extracted from 25 μL of serum following protein precipitation using 100 μL of 2:1 chloroform/methanol (v/v). Samples were vortex-mixed and centrifuged for 10 min at 10 000g and 4 °C. The bottom phase was collected, dried, and resuspended in 100 μL of 50:50 acetonitrile/isopropanol (v/v) for further MS analysis. Total lipid analysis was performed on an IonKey/MS system composed of an ACQUITY UPLC M-Class, the ionKey source, and an iKey CSH C18, 130 Å, 1.7 μm (particle size), 150 μm × 100 mm column (Waters Corporation, Milford, MA, USA) coupled to a Synapt G2-Si mass spectrometer (Waters Corporation, Wilmslow, UK). The capillary voltage was 2.8 kV, and the source temperature was 110 °C. Injections were 0.5 μL using the partial-loop mode, and the column temperature and flow rate were 55 °C and 3 μL/min, respectively. Mobile phase A consisted of 60:40 acetonitrile/water (v/v) with 10 mM ammonium formate + 0.1% formic acid. Mobile phase B consisted of 90:10 isopropanol/acetonitrile (v/v) with 10 mM ammonium formate + 0.1% formic acid. The gradient was programmed as follows: 0.0−2.0 min from 40% B to 43% B, 2.0−2.1 min to 50% B, 2.1−12.0 min to 99% B, 12.0−12.1 min to 40% B, and 12.1−14.0 min at 40% B. A 3 min re-equilibration time was applied. MS analyses were performed, acquiring from 50 to 1500 m/z in positive electrospray ionization mode with a capillary voltage of 2.8 kV. Data were collected in two channels all of the time: low collision energy (6.0 V), for the molecular ions, and high collision energy (15−40 V), for product ions. The IMS gas was nitrogen, and the IMS T-Wave velocity and height were 900 m/s and 40 V, respectively.

Targeted Metabolic Profiling

Metabolites were extracted from mice sera using a specific 96-well plate system for protein removal, internal standard normalization, and derivatization using the Absolute IDQ p180 Kit (Biocrates Life Sciences AG, Innsbruck, AUT). The methods have been described in detail,[29,30] and the preparation was performed according to the user manual included with the kit. Briefly, 10 samples ($n = 5$ sham-irradiated group and $n = 5$ irradiated group) were added to the center of the filter on the upper 96-well kit plate, at 10 μL per well, and then dried using a nitrogen evaporator. Subsequently, 50 μL of a 5% solution of phenylisothiocyanate was added for derivatization of the amino acids and biogenic amines. After incubation, the filter spots were dried again using a nitrogen evaporator. The metabolites were extracted using 300 μL of a 5 mM ammonium acetate solution in methanol and transferred by centrifugation into the lower 96-well plate.

The extracts were diluted with 600 μL of the MS running solvent for further MS analysis using UPLC coupled with the Xevo TQ-S mass spectrometer (Waters Corporation, Wilmslow, UK). Instrument conditions are detailed in Table S1. One blank sample (i.e., no internal standards and no sample added), three water-based zero samples (phosphate-buffered saline), and three quality-control samples were also added to the kit plate. The quality control samples, composed of human serum containing
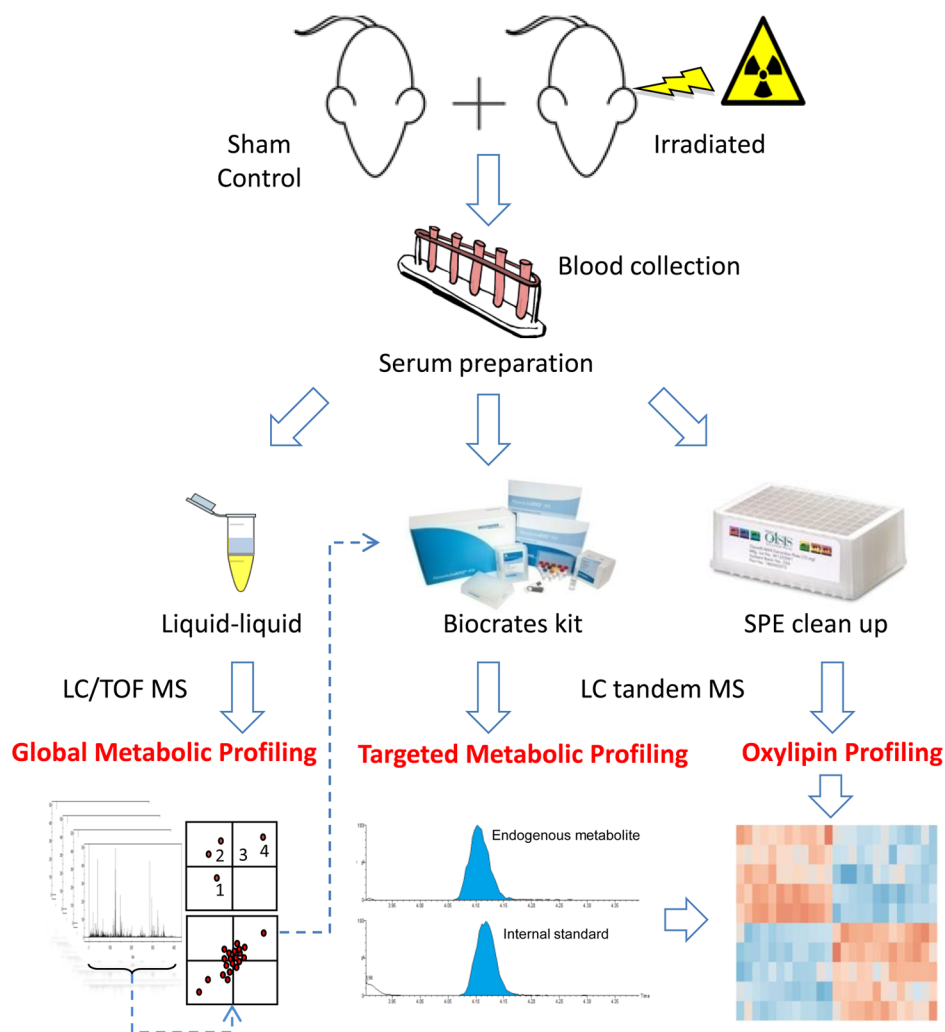
Figure 1. Study design and workflow for the metabolic phenotyping. CB57Bl/6 mice were irradiated (8 Gy; $n = 5$) or subjected to the same treatment minus irradiation (sham control group; $n = 5$). Blood was collected, and serum samples were prepared and divided into two aliquots. Before extraction, a mixture of internal standards was added to the serum to normalize for variations in sample preparation or MS detection. Initial discovery data were further investigated using complementary multiplexed metabolic-profiling approaches. The results were integrated for the generation of a unique metabolic biosignature, which indicates exposure to radiation.

metabolites at several concentration levels, were used to verify the performance of the assay and mass spectrometer. A seven-point serial dilution of calibrators was added to the kit's 96-well plate to generate calibration curves used to quantify biogenic amines and amino acids. The kit included a mixture of internal standards for quantifying the natural metabolites: chemical homologous internal standards were used to quantify glycerophospholipid and sphingomyelin species, whereas stable isotope-labeled internal standards were used to quantify the other compound classes. The amount of internal standards was identical in each well, and the internal-standard intensities of zero sample and sample wells were compared to allow conclusions on ion-suppression effects to be made. Acylcarnitines, glycerophospholipids, and sphingolipids were subjected to flow-injection analysis (FIA) using UPLC-Xevo TQ-S in positive mode. Hexose was analyzed using a subsequent FIA acquisition in negative electrospray ionization mode. Amino acids and biogenic amines were analyzed using an ACQUITY UPLC system connected to a Xevo TQ-S mass spectrometer (Waters Corporation, Wilmslow, UK) in positive electrospray ionization mode (Table S1).

Targeted Oxylipins Profiling

Extraction of oxylipins was performed as previously described.[31] Briefly, after thawing on ice, 50 μL of serum samples was treated immediately with antioxidants (0.2 mg butylated hydroxytoluene (BHT/EDTA)) and spiked with the following internal standards: 6k-PGF$_{1\alpha}$-d_4, TXB$_2$-d_4, PGF$_2\alpha$-d_4, PGE2-d_4, PGD$_2$-d_4, LTE$_4$-d_3, LTB$_4$-d_4, 12,13 diHOME-d_4, 9,10-diHOME-d_4, 14,15-DiHETrE-d11, 15-deoxy-δ-12,14-PGJ$_2$-d_4, 20-HETE-d_6, 9S-HODE-d_4, 12S-HETE-d_8, 5S-HETE-d_8, 5-oxo-ETE-d_7. Serum samples were loaded onto the solid-phase extraction plate and then eluted using 1.5 mL of ethyl acetate after wetting the plate wells with 0.5 mL of methanol. The eluent was reduced under nitrogen and subsequently reconstituted in a 50 μL solution of 50:50 methanol/acetonitrile (v/v) containing 100 nM 1-cyclohexyluriedo-3-dodecanoic acid, a quality marker for the analysis.

Oxylipins were analyzed using UPLC (Waters Corporation, Milford, MA, USA) coupled to electrospray ionization on a Xevo TQ-S mass spectrometer (Waters Corporation, Wilmslow, UK). The autosampler was cooled to 10 °C. For each analysis, 3 μL of sample was injected onto a BEH C18 1.7 μm, 2.1 × 100 mm

Table 1. Tentative Identification of Lipid Alterations Obtained from a Global Metabolic Profiling[a]

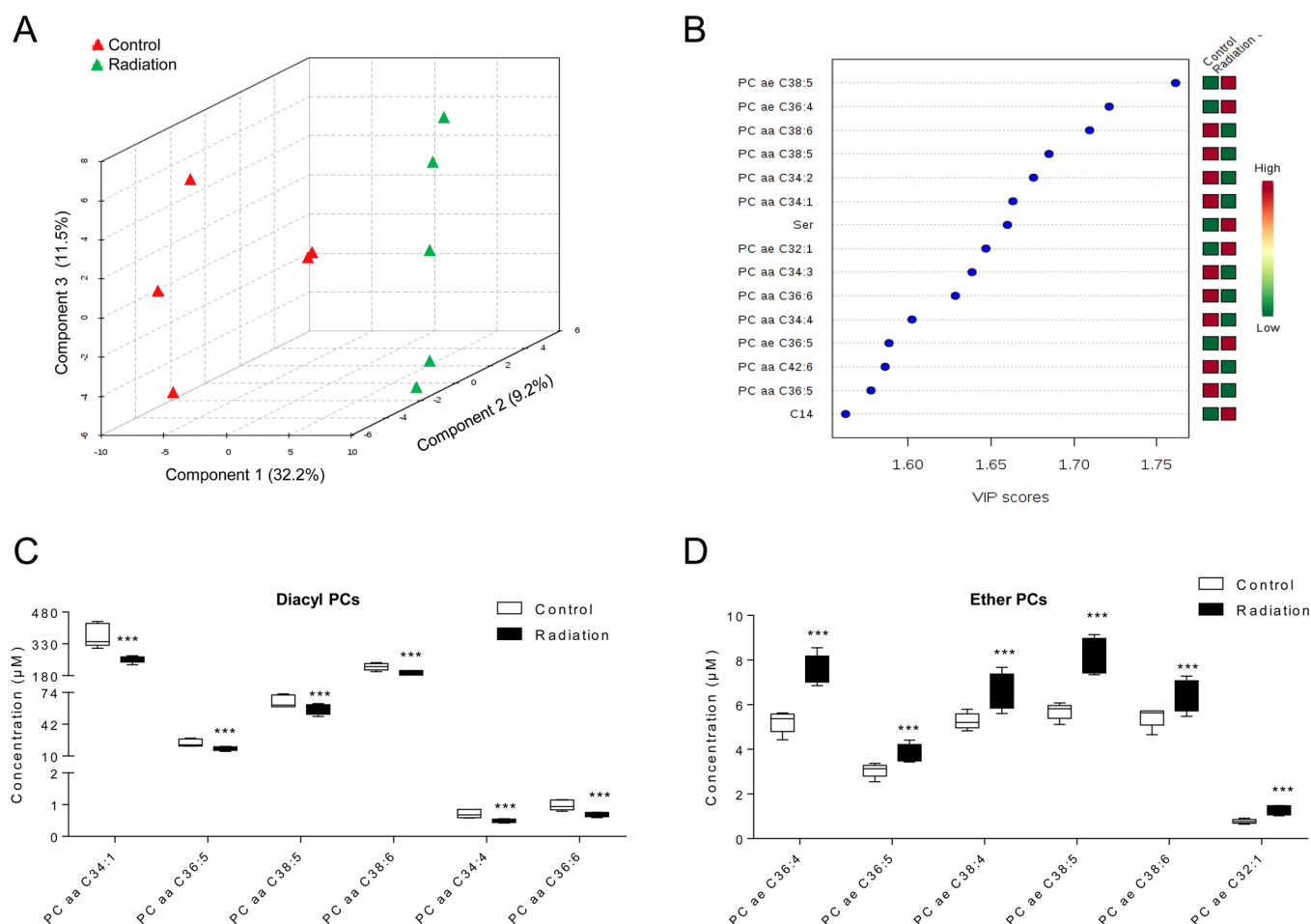| m/z	tentative ID	ANOVA (p value)	max fold change	method
818.6050	PC(P-18:0/22:6)	5.12×10^{-6}	8.0	reversed phase
764.5571	PC(P-16:0/20:5)	1.02×10^{-5}	11.3	reversed phase
804.5529	PC(P-16:0/20:4)	2.11×10^{-5}	9.8	reversed phase
794.6038	PC(P-18:0/20:4)	2.97×10^{-5}	5.7	reversed phase
792.5873	PC(P-18:0/20:5)	3.38×10^{-5}	8.1	reversed phase
790.5728	PC(P-16:0/22:6)	6.74×10^{-5}	5.9	reversed phase
703.5747	SM(d18:1/16:0)	2.09×10^{-4}	12.5	reversed phase
162.1117	carnitine	1.50×10^{-2}	1.7	HILIC
166.0861	phenylalanine	1.53×10^{-2}	1.2	HILIC

[a]Lipids are ranked according to their ANOVA p values.

column (Waters Corporation, Milford, MA, USA) maintained at 40 °C. The flow rate was 0.6 mL/min. Mobile phases were composed as follows: A = 0.1% acetic acid and B = 90:10 (v/v) acetonitrile/isopropanol (0.00−1.00 min from 25% B to 33% B, 1.01−8.00 min B to 95%, 8.01−8.50 min to 95% B, 8.51−10.00 min to 25% B). Electrospray ionization was performed in the negative-ion mode applying a capillary voltage of 2 kV, a source temperature of 120 °C, a desolvation gas temperature of 350 °C, a desolvation gas flow of 650 L/h, a cone-gas flow of 150 L/h, a

collision voltage of 15 V, and a cone voltage of 35 V. Oxylipins were detected by means of multiple reaction monitoring (MRM) transitions optimized using synthetic standards (Table S2). Limits of quantification were in the lower picomolar range.

Data Processing and Analysis

For global molecular profiling, samples were acquired as ion maps (retention time versus m/z) using data-independent analysis (MS^E), which provided information for both the intact precursor ions (at low collision energy) and the fragment ions (high collision energy). After retention-time alignment, an aggregate run representing the compounds in all samples was generated. This aggregate run was used for peak picking and then propagated to all runs to detect the same ions in each. A combination of analysis of the variance (ANOVA) including principal component analysis (PCA) and partial, least-squares discriminant analysis (PLS-DA) identified metabolites most responsible for differences between sample groups. Compounds were identified by database searches. These searches were performed by the Human Metabolome Database (HMDB)[32] and LipidMaps and by fragmentation patterns, retention times, and ion-mobility-derived collision cross sections versus commercially available reference standards, when available. For quantification purposes, mean concentrations and SEM values
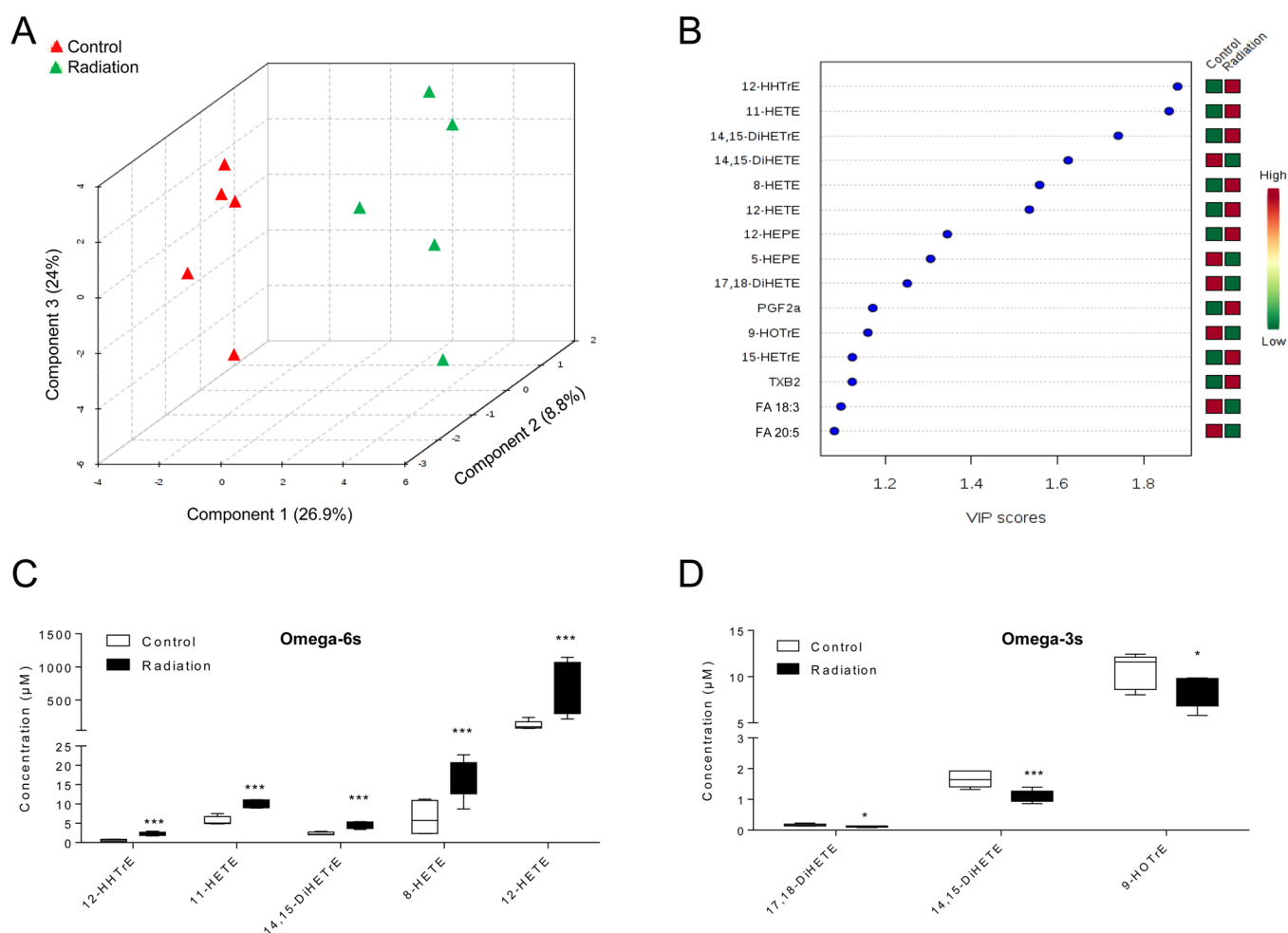

Figure 2. Targeted metabolic profiling. (A) PLS-DA analysis showed a marked separation of serum metabolites belonging to irradiated and sham control mice, highlighting the features that contributed most to the variance between the two groups. (B) Important features identified by PLS-DA. The colored boxes on the right indicate the relative concentrations of the corresponding metabolite in each group under study. The variable importance in projection (VIP), a weighted sum of squares of the PLS loadings, takes into account the amount of explained Y variation in each dimension. (C, D) Levels of diacyl PCs (C) and ether PCs (D) in irradiated and sham control (n = 5, Student's t test; ***, p < 0.001). The data represent the mean ± SEM.

Figure 3. Targeted oxylipin profiling. (A) PLS-DA analysis showed a marked separation of serum oxylipins belonging to irradiated and sham control mice, highlighting the features that contributed most to the variance between the two groups. (B) Important features identified by PLS-DA. The colored boxes on the right indicate the relative concentrations of the corresponding metabolite in each group under study. Variable importance in projection (VIP), a weighted sum of squares of the PLS loadings, takes into account the amount of explained Y variation in each dimension. (C, D) Levels of omega-6 oxylipins (C) and omega-3 oxylipins (D) in irradiated and sham control mice ($n = 5$, Student's t test; *, $p < 0.05$; ***, $p < 0.001$). The data represent the mean ± SEM.

RESULTS

for each group were calculated using MRM transition and appropriate internal standards to normalize for variations in sample preparation and MS detection. Univariate analyses (Student's t-test) were conducted to assess for significance (p value < 0.05 was considered significant), and false-discovery rate (FDR) was used to control for multiple comparison.

Data processing and analysis was conducted using Progenesis QI (Nonlinear Dynamics, Newcastle, UK), MetaboLyzer,[33] and MetaboAnalyst 2.0.[34] Data quantification was performed using TargetLynx software (Waters Corporation, Milford, MA, USA) and MetIDQ software (Biocrates Life Sciences AG, Innsbruck, AUT).

■ RESULTS

To characterize the molecular response associated with exposure to radiation, we phenotyped the metabolomes of irradiated mice (8 Gy, $LD_{50/30}$) and sham control mice using a multiplatform mass spectrometry-based approach (Figure 1). Serum metabolomes from sham control and irradiated mice were subjected to global metabolic profiling to screen for major molecular alterations. Identification and quantification of bioactive and low-abundance metabolites followed (Figure 1). The overall effects on blood cell levels in combination with various

symptoms associated with the acute radiation syndrome following exposure to a $LD_{50/30}$ have been described extensively in the literature.[35,36]

To determine the overall effect of radiation on the molecular phenotype, we compared the serum metabolome of sham control and irradiated mice using a microfluidic device coupled with an electrospray-TOF detector, detecting thousands of molecular features in serum samples (Figure S1). PCA showed that the γ-irradiated group was well-separated from the sham control group, underscoring that radiation induces a profound molecular response in blood. Significant changes were filtered using ANOVA, highlighting the molecular features that contributed most to the variance between the two groups of mice (Figure S1). Among the dysregulated molecular components, we tentatively identified metabolites belonging to the classes of amino acids, carnitines, sphingomyelins, and phosphatidylcholines as discriminators of the sham control and irradiated groups (Table 1).

To further investigate these initial findings, in an independent set of experiments, we applied a multiplexed metabolic profiling approach. Using stable-isotope-dilution tandem MS, we identified and quantified more than 180 endogenous metabolites

Table 2. Levels of Detected Oxylipins Expressed as Mean Concentration (pmol/mL) and SEM Values (n = 5) for Sham Control and Irradiated Groups[a]

oxylipin	mean (sham control)	SEM	mean (irradiated)	SEM	p value	FDR
12-HHTrE	0.63	0.45	2.26	0.60	0.000108	0.003439
11-HETE	5.67	0.94	10.13	0.91	0.000176	0.003439
14,15-DiHETrE	2.35	0.54	4.39	0.84	0.001414	0.01838
14,15-DiHETE	1.66	0.46	1.10	0.40	0.005186	0.050566
8-HETE	6.48	1.86	16.66	2.02	0.009194	0.071715
12-HETE	117.40	7.35	725.74	18.07	0.011043	0.071779
12-HEPE	35.53	4.08	228.56	11.68	0.036213	0.20176
5-HEPE	3.03	0.86	2.03	0.41	0.044053	0.21476
17,18-DiHETE	3.30	0.78	2.42	0.61	0.056722	0.2458
PGF2a	3.04	0.88	4.52	1.03	0.079585	0.287
9-HOTrE	10.60	1.23	8.38	1.15	0.08325	0.287
15-HETrE	2.40	0.80	3.51	0.91	0.095583	0.287
TXB2	1.21	0.74	3.62	1.49	0.095668	0.287
FA 18:3 (alpha-linolenic acid omega-3)	36.50	2.25	30.90	1.47	0.10532	0.28922
FA 20:5 omega-3 (EPA)	23.75	1.30	21.48	1.23	0.11124	0.28922
13-KODE	19.82	2.17	30.03	3.11	0.12822	0.31253
9-KODE	17.59	1.43	24.31	2.70	0.15088	0.34001
15-HETE	1.98	0.63	2.56	0.72	0.15693	0.34001
9-HODE	87.20	3.33	73.09	3.72	0.19229	0.39471
FA 18:2 (linoleic acid omega-6)	53.18	2.97	45.72	2.10	0.21301	0.41536
12(13)-EpOME	33.94	2.43	28.15	2.45	0.25357	0.4593
12,13-DiHOME	310.64	6.10	271.19	6.68	0.25909	0.4593
PGE2	0.67	0.36	0.81	0.43	0.3001	0.49635
19,20-DiHDPA	2.88	0.86	3.50	0.83	0.30545	0.49635
FA 22:6 (DHA)	34.00	1.78	31.92	1.60	0.38721	0.60405
17-HDoHE	2.35	1.72	4.04	1.51	0.43961	0.65942
20-HETE	1.90	0.66	2.40	1.04	0.46462	0.67112
9(10)-EpOME	43.26	1.97	46.39	3.05	0.59375	0.77352
9,10-DiHOME	156.45	4.17	148.00	4.63	0.59936	0.77352
15-HEPE	1.45	0.71	1.65	0.66	0.60528	0.77352
5-HETE	5.82	1.02	5.29	1.23	0.61485	0.77352
15-KETE	3.05	0.54	3.44	1.20	0.64769	0.78937
FA 20:3 omega-6	5.24	0.72	5.03	0.90	0.70917	0.83811
9-HpODE	2.53	0.68	2.70	0.85	0.73504	0.84314
FA 20:4 (arachidonic acid)	29.44	1.75	29.97	1.86	0.84414	0.91663
15-deoxy-alpha 12,14-PGD2	3.49	0.97	4.03	2.17	0.84612	0.91663
(±) 5-iPF2a-VI	1.95	0.65	1.88	0.83	0.88401	0.93179
PGF1a	3.26	1.11	3.32	0.94	0.94491	0.96978
13-HODE	217.02	5.60	217.98	8.22	0.98217	0.98217

[a]Oxylipins are ranked according to their Student's t-test p values. FDR, false discovery rate.

from six biochemical classes: biogenic amines, amino acids, glycerophospholipids, sphingolipids, sugars, and acylcarnitines (Table S3). Multivariate statistical analyses showed that exposure to γ radiation induced significant molecular changes in mouse sera (Figure 2A,B and Figure S2A). In particular, we observed a decrease in the levels of diacyl phosphatidylcholines (PCs) containing polyunsaturated fatty acids (PUFAs) (Figure 2C and Table S3) but a significant increase in the levels of ether PCs in mice exposed to radiation compared with that in their sham-irradiated littermates (Figure 2D and Table S3). Moreover, in the irradiated animals, the levels of lysophosphatidylcholines and sphingomyelins (SM) were also increased (Table S3). Such differences were found to be significant after multiple-comparison correction (FDR < 0.01). Other significant differences between sham control and irradiated mice included the levels of serine and carnitines, which increased after irradiation (Figure 2B and Table S3).

PC species can be hydrolyzed to release PUFAs that can then be converted into oxylipins by means of enzymatic and nonenzymatic reactions. To measure the levels of such, usually, low-abundance metabolites, we used a tandem MS with multiple reaction monitoring for over 100 oxylipins (Figure 1). The overall oxylipins composition was sufficient to discriminate between irradiated and sham control animals (Figure S2B and Figure 3A,B). We observed a marked increase in the levels of arachidonic acid-derived metabolites (Figure 3B and Table 2). In particular, a significant increase after multiple comparison correction was found for hydroxyeicosatetraenoic acids (12-HETE, 11-HETE, 8-HETE), 14,15 dihydroxy-eicosatrienoic acid (14,15-DiHETrE), and 12-hydroxy-heptadecatrienoic acid (12-HHTrE) in mice exposed to radiation versus that in the sham control animals (Figure 3C and Table 2). Our results also highlighted a marked decrease in the levels of diols of EPA including 17,18-DiHETE and 14,15-DiHETE in the serum of mice exposed to radiation versus that in the serum of sham-treated mice (Figure 3D and Table 2).
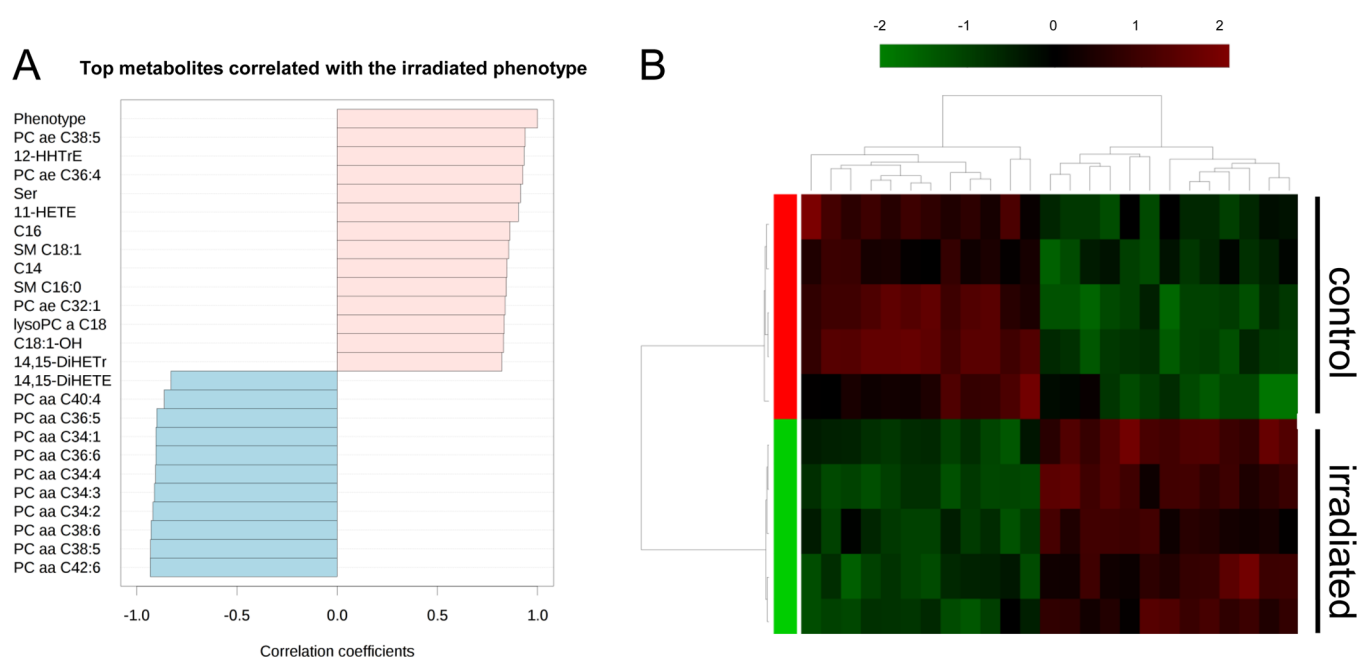
Figure 4. Lipidomic biosignature of irradiated mice. (A) Correlation analysis was used to visualize the overall relationships between different features and the irradiated phenotype. (B) Clustering result shown as a heatmap (distance measure using Pearson; clustering algorithm using Ward) providing an intuitive visualization of the characteristic lipidomic biosignature found in irradiated mice versus sham control mice. Each colored cell on the map corresponds to a concentration value, with samples in rows and features/compounds in columns. Displayed are the top 25 lipids, ranked by Student's t tests.

Minor decreases were also observed for other ALA- or DHA-derived metabolites (Figure 3B and Table 2).

To obtain a metabolic biosignature of mice that would indicate radiation exposure, we combined the quantitative results derived from the multiplexed metabolic profiling analyses, underscoring a significant molecular contrast between sham control and irradiated mice (Figure 4A,B). The sham control molecular composition exhibits a decidedly distinct pattern and structure compared with that of the irradiated one, suggesting that radiation elicits a very distinct metabolic response (Figure S3).

DISCUSSION

In this study, we investigated the molecular response to radiation exposure in mice using a multiplatform mass spectrometry-based strategy. We phenotyped the serum of irradiated and sham control mice, reporting novel metabolic pathways altered after radiation exposure. Most of the study's novelty resides in the finding that radiation induces a differential regulation of diacyl PCs and ether PCs as well as omega-6 and omega-3 lipid mediators. Such radiation-induced changes in lipid composition could have repercussions on (1) the physicochemical properties of cellular membranes and lipoproteins, (2) the cellular antioxidant buffering capacity, and (3) cell signaling. Many of these molecular changes may not be specific to the radiation exposure but act instead as general makers of cellular/organism stress and inflammation.

Limited studies have investigated the effects of ionizing radiation on the blood level of metabolites and lipids in particular.[15,23,25,37−39] It is reported that treatment of lipid membranes with ionizing radiation leads to lipid degradation, which is mediated by both oxidation and fragmentation processes.[16] Such studies, however, aimed to measure the content of a limited number of lipid metabolites in reductionistic models such as synthetic lipid membranes and cellular models.

By using a multiplatform mass spectrometry-based approach, we were able to describe in a more comprehensive fashion the alterations in the molecular phenotype of mouse serum following irradiation. In our study, we analyzed metabolites with a wide dynamic range of concentrations: from low-abundance oxylipins, in the picomolar range, to the higher abundance precursor phospholipids, in micromolar amounts.

The observed phospholipids rearrangement, a decrease in the levels of diacyl PC species and an increase in ether PCs (plasmalogens), might ultimately have repercussions on the physicochemical properties of the cellular membranes and lipoproteins.[40−42] The phospholipid class of plasmalogens is indeed ubiquitously found in considerable amounts as a constituent of mammalian cell membranes and of serum lipoproteins. Plasmalogens are more susceptible than diacyl PCs to oxidative reactions because of the reactivity of their enol-ether function; indeed, it is reported that they are effective as endogenous antioxidants.[42−45] Oxidation of the vinyl ether markedly prevents the oxidation of highly polyunsaturated fatty acids, and products of plasmalogen degradation do not propagate lipid oxidation. On the other hand, the oxidation of the vinyl ether bond of plasmalogens leads to the release of fatty aldehydes, which are toxic to cells.[44,46] The pathological role of plasmalogens and the biochemical pathways underlying their upregulation after radiation exposure remain to be elucidated.[47]

The most intriguing observation of our study is that acute exposure to γ radiation induced a specific mobilization of bioactive oxylipins (Figure 5A,B). These lipid mediators are currently the focus of considerable interest, for they are also key messengers for cellular homeostasis, inflammation, platelet aggregation, and vascularization.[48−52] Oxylipins are produced via enzymatic or nonenzymatic oxygenation of both omega-6 and omega-3 PUFAs. Three major enzymatic pathways are involved in their generation: cyclooxygenase (COX), lipoxygenase (LOX), and cytochrome P450 (CYP450) (Figure 5A,B).

Figure 5. Pathway analysis. Diet-derived omega-6 linoleic acid (LA) and omega-3 alpha-linolenic acid (ALA) are transformed into longer chains PUFAs by the sequential action of desaturases and elongases. PUFAs can be found in blood as unesterified fatty acids, esterified to phospholipids, or converted into the oxygenated metabolites oxylipins. (A, B) The activities of COX, LOX, and CYP450 enzymes catalyze the formation of hundreds of oxylipins species with different biological activities starting from the omega-6 PUFAs precursors (A) and the omega-3 PUFAs (B). The irradiated mice had marked alterations in the LOX, COX, and CYP450 pathways, resulting in the increase of omega-6 oxylipins (red) and decrease of omega-3 oxylipins (green).

Significantly, it is reported that ionizing radiation activates COX and LOX pathways and that nonsteroidal anti-inflammatory drug treatment reduces radiation-induced expression of pro-inflammatory cytokines (e.g., TNF-α, TGF-β, IL-6, and IL-1 α/β).[53−55] In agreement with these observations, our results further suggest that oxylipins-mediated inflammation might be a

critical signaling step for the organism response to radiation. Macrophage activation leading to a persistent inflammatory response has been described in radiation therapy for cancer[28,56,57] in animals following irradiation[56] and in atomic bomb survivors.[58,59] Like other inflammatory cytokines, oxylipins are major components of immediate-early gene programs. As such, they can be rapidly activated after tissue irradiation as part of the immune response to stress factors and thus they might disrupt cellular homeostasis over time, causing detrimental health effects.[60] It is therefore reasonable to speculate that oxylipins-mediated inflammation could be involved in the bystander and abscopal effects associated with clinical exposures to ionizing radiation in a radiotherapy-type situation.[53,55,61−63]

Our study indicates that 24 h following irradiation omega-6 pro-inflammatory lipid mediators derived from the COX and LOX pathways (e.g., HETEs, PGF2α, TBX2) are upregulated, while the levels of omega-3 anti-inflammatory mediators (e.g., 5-HEPE, 9-HoTrE) are downregulated. Notably, some of the most significant oxylipins alterations in the serum of irradiated mice were related to the metabolism of the CYP450 pathway, including 14,15-DiHETrE, 14,15-DiHETE, and 17,18-DiHETE (Figure 5). The CYP450 family of enzymes can produce epoxides from PUFAs, which are subsequently metabolized by the soluble epoxide hydrolase (sEH) to the corresponding vicinal diols, dihydroxyeicosatrienoic acids.[64,65] AA-derived CYP metabolites are known to play an important role in renal and cardiovascular function and are linked to the development of hypertension and related disease.[66−68] Omega-3 PUFA-derived CYP metabolites are described as possessing anti-inflammatory[69] and analgesic properties,[70] as inhibitors of platelet aggregation,[71] and as pulmonary smooth-muscle relaxants.[72] Our results support the hypothesis that CYP450-mediated oxylipins metabolism might represent a major biochemical pathway in response to acute exposure to ionizing radiation. Most notably, in human and animal studies, the CYP-dependent metabolite profiles were generally reflective of the PUFA intake,[64,73−78] suggesting the use therapeutic interventions designed to modulate the levels of oxylipins as a preventive measure or as a countermeasure to cope with the debilitating effects of radiation exposure.[78]

Oxylipins levels might greatly affect intrinsic cellular radiosensitivity, the incidence and type of radiation-induced tissue complications, and diseases.[79,80] The balance between omega-6 pro-inflammatory and omega-3 anti-inflammatory lipid mediators may play a key role in the different phases of the response to radiation: a pro-inflammatory phase followed by a pro-resolution phase to restore cellular homeostasis.[48,81,82] Notably, it is reported that an unbalanced inflammatory response resulting as a consequence of radiation exposure might contribute to both cancer and non-cancer-related diseases, including eye and brain diseases[5,6] and cardiovascular disease.[7−13] Therefore, the ability to control oxylipin pathways with dietary interventions (i.e., omega-3 supplementation) might alleviate and eventually offset many of the side effects linked to either radiation therapy or accidental exposure.[78,82−84]

Notably, the most significant molecular alterations induced by exposure to radiation affected lipid metabolism. Our study, however, also reports a dysregulation of the metabolism of amino acids (e.g., serine) and carnitines (Figure 4 and Table S3) in mice exposed to radiation. Such findings, together with more modest alterations of intermediates of the urea cycle (e.g., citrulline, FDR = 0.05), were previously reported and linked to radiation-induced gastrointestinal and liver damage.[20,22,23,85−87] By offering a bird's eye view of the molecular response to radiation exposure, our study highlights the interplay between lipid metabolism and the network of biochemical pathways for more polar metabolites, which is an object of continued and renewed investigation by the scientific community.

■ CONCLUSIONS

Using a metabolic phenotyping approach, we identified a novel molecular response in mouse serum following exposure to γ radiation. The integration of metabolic profiling information provided a detailed molecular biosignature that might be used as an indicator of radiation exposure and, potentially, as a predictor of radiosensitivity. Most important, the molecular components identified in the present study (i.e., plasmalogens and oxylipins) would enable us to modulate their levels using currently available pharmacological treatments or nutritional intervention.

If validated in humans, our findings could find applications in personalized medicine. Numerous attempts have been made to develop DNA-based diagnostic assays to identify cancer patients who might develop severe adverse healthy tissue reactions in response to radiotherapy.[88−91] We speculate that baseline levels of oxylipins (e.g., omega-6/omega-3 ratio) might serve as a companion diagnostic tool for radiation therapy to help differentiate cancer patients who would respond best to radiotherapy treatment from radiosensitive patients who may be unable to tolerate the additional inflammatory response induced by radiotherapy.[78,92,93]

■ ASSOCIATED CONTENT

Ⓢ Supporting Information

Instrument parameters for the targeted metabolic profiling; retention times, monitored transitions, and internal standards used for oxylipins quantification; levels of metabolites expressed as mean concentration and SEM values for non-irradiated and irradiated mice; workflow for the global metabolic profiling analysis; multivariate statistical analyses of multiplexed, metabolic data sets; and correlation heatmaps. This material is available free of charge via the Internet at http://pubs.acs.org.

■ AUTHOR INFORMATION

Corresponding Author

*E-mail: giuseppe_astarita@waters.com.

Notes

The authors declare no competing financial interest.

■ ACKNOWLEDGMENTS

■ ABBREVIATIONS

IMS, ion mobility spectrometry; FDR, false discovery rate; VIP, very important features; PLS-DA, partial, least-squares discriminant analysis; PCA, principal component analysis; COX, cyclooxygenase; LOX, lipoxygenase; CYP450, cytochrome P450; DiHETE, dihydroxy-eicosatetraenoic acid; HEPE, hydroxy-eicosapentaenoic acid; HETrE, hydroxy-eicosatrienoic acid; oxo-ETE, oxo-eicosatetraenoic acid; EpETE, epoxy-eicosatetraenoic acid; bicyclo-PGE2, bicyclo-prostaglandin E2; BHT, butylated hydroxytoluene; IL-β, interleukin-1 beta; IL-6, interleukin 6; LA, inoleic acid; ALA, alpha-linolenic acid; DHA,

docosahexaenoic acid; AA, arachidonic acid; DGLA, dihomo-γ-linolenic acid; EPA, eicosapentaenoic acid; LT, leukotriene

■ REFERENCES

(1) Brenner, D. J.; Hall, E. J. Computed tomography—an increasing source of radiation exposure. *N. Engl. J. Med.* **2007**, *357*, 2277–84.

(2) Pearce, M. S.; Salotti, J. A.; Little, M. P.; McHugh, K.; Lee, C.; Kim, K. P.; Howe, N. L.; Ronckers, C. M.; Rajaraman, P.; Sir Craft, A. W.; Parker, L.; Berrington de Gonzalez, A. Radiation exposure from CT scans in childhood and subsequent risk of leukaemia and brain tumours: a retrospective cohort study. *Lancet* **2012**, *380*, 499–505.

(3) Mathews, J. D.; Forsythe, A. V.; Brady, Z.; Butler, M. W.; Goergen, S. K.; Byrnes, G. B.; Giles, G. G.; Wallace, A. B.; Anderson, P. R.; Guiver, T. A.; McGale, P.; Cain, T. M.; Dowty, J. G.; Bickerstaffe, A. C.; Darby, S. C. Cancer risk in 680,000 people exposed to computed tomography scans in childhood or adolescence: data linkage study of 11 million Australians. *BMJ* **2013**, *346*, f2360.

(4) Miglioretti, D. L.; Johnson, E.; Williams, A.; Greenlee, R. T.; Weinmann, S.; Solberg, L. I.; Feigelson, H. S.; Roblin, D.; Flynn, M. J.; Vanneman, N.; Smith-Bindman, R. The use of computed tomography in pediatrics and the associated radiation exposure and estimated cancer risk. *JAMA Pediatr* **2013**, *167*, 700–7.

(5) Ozasa, K.; Shimizu, Y.; Sakata, R.; Sugiyama, H.; Grant, E. J.; Soda, M.; Kasagi, F.; Suyama, A. Risk of cancer and non-cancer diseases in the atomic bomb survivors. *Radiat. Prot. Dosim.* **2011**, *146*, 272–5.

(6) Picano, E.; Vano, E.; Domenici, L.; Bottai, M.; Thierry-Chef, I. Cancer and non-cancer brain and eye effects of chronic low-dose ionizing radiation exposure. *BMC Cancer* **2012**, *12*, 157.

(7) Baker, J. E.; Moulder, J. E.; Hopewell, J. W. Radiation as a risk factor for cardiovascular disease. *Antioxid. Redox Signaling* **2011**, *15*, 1945–56.

(8) Yan, X.; Sasi, S. P.; Gee, H.; Lee, J.; Yang, Y.; Song, J.; Carrozza, J.; Goukassian, D. A. Radiation-associated cardiovascular risks for future deep-space missions. *J. Radiat. Res.* **2014**, *55*, i37–i39.

(9) Shimizu, Y.; Kodama, K.; Nishi, N.; Kasagi, F.; Suyama, A.; Soda, M.; Grant, E. J.; Sugiyama, H.; Sakata, R.; Moriwaki, H.; Hayashi, M.; Konda, M.; Shore, R. E. Radiation exposure and circulatory disease risk: Hiroshima and Nagasaki atomic bomb survivor data, 1950–2003. *BMJ* **2010**, *340*, b5349.

(10) Zielinski, J. M.; Ashmore, P. J.; Band, P. R.; Jiang, H.; Shilnikova, N. S.; Tait, V. K.; Krewski, D. Low dose ionizing radiation exposure and cardiovascular disease mortality: cohort study based on Canadian national dose registry of radiation workers. *Int. J. Occup. Med. Environ. Health* **2009**, *22*, 27–33.

(11) Little, M. P.; Tawn, E. J.; Tzoulaki, I.; Wakeford, R.; Hildebrandt, G.; Paris, F.; Tapio, S.; Elliott, P. Review and meta-analysis of epidemiological associations between low/moderate doses of ionizing radiation and circulatory disease risks, and their possible mechanisms. *Radiat. Environ. Biophys.* **2010**, *49*, 139–53.

(12) Rodel, F.; Frey, B.; Manda, K.; Hildebrandt, G.; Hehlgans, S.; Keilholz, L.; Seegenschmiedt, M. H.; Gaipl, U. S.; Rodel, C. Immunomodulatory properties and molecular effects in inflammatory diseases of low-dose X-irradiation. *Front. Oncol.* **2012**, *2*, 120.

(13) Rodel, F.; Keilholz, L.; Herrmann, M.; Sauer, R.; Hildebrandt, G. Radiobiological mechanisms in inflammatory diseases of low-dose radiation therapy. *Int. J. Radiat. Biol.* **2007**, *83*, 357–66.

(14) Coy, S. L.; Cheema, A. K.; Tyburski, J. B.; Laiakis, E. C.; Collins, S. P.; Fornace, A., Jr. Radiation metabolomics and its potential in biodosimetry. *Int. J. Radiat. Biol.* **2011**, *87*, 802–23.

(15) Dainiak, N.; Tan, B. J. Utility of biological membranes as indicators for radiation exposure: alterations in membrane structure and function over time. *Stem Cells* **1995**, *13*, 142–52.

(16) Shadyro, O. I.; Yurkova, I. L.; Kisel, M. A. Radiation-induced peroxidation and fragmentation of lipids in a model membrane. *Int. J. Radiat. Biol.* **2002**, *78*, 211–7.

(17) Lanz, C.; Patterson, A. D.; Slavik, J.; Krausz, K. W.; Ledermann, M.; Gonzalez, F. J.; Idle, J. R. Radiation metabolomics. 3. Biomarker discovery in the urine of gamma-irradiated rats using a simplified metabolomics protocol of gas chromatography-mass spectrometry

combined with random forests machine learning algorithm. *Radiat. Res.* **2009**, *172*, 198–212.

(18) Guipaud, O. Serum and plasma proteomics and its possible use as detector and predictor of radiation diseases. *Adv. Exp. Med. Biol.* **2013**, *990*, 61–86.

(19) Hyduke, D. R.; Laiakis, E. C.; Li, H. H.; Fornace, A. J., Jr. Identifying radiation exposure biomarkers from mouse blood transcriptome. *Int. J. Bioinf. Res. Appl.* **2013**, *9*, 365–85.

(20) Cheema, A. K.; Suman, S.; Kaur, P.; Singh, R.; Fornace, A. J., Jr.; Datta, K. Long-term differential changes in mouse intestinal metabolomics after gamma and heavy ion radiation exposure. *PLoS One* **2014**, *9*, e87079.

(21) Goudarzi, M.; Weber, W.; Mak, T. D.; Chung, J.; Doyle-Eisele, M.; Melo, D.; Brenner, D. J.; Guilmette, R. A.; Fornace, A. J. Development of urinary biomarkers for internal exposure by cesium-137 using a metabolomics approach in mice. *Radiat. Res.* **2014**, *181*, 54–64.

(22) Laiakis, E. C.; Mak, T. D.; Anizan, S.; Amundson, S. A.; Barker, C. A.; Wolden, S. L.; Brenner, D. J.; Fornace, A. J. Development of a metabolomic radiation signature in urine from patients undergoing total body irradiation. *Radiat. Res.* **2014**, *181*, 350–61.

(23) Jones, J. W.; Scott, A. J.; Tudor, G.; Xu, P. T.; Jackson, I. L.; Vujaskovic, Z.; Booth, C.; MacVittie, T. J.; Ernst, R. K.; Kane, M. A. Identification and quantitation of biomarkers for radiation-induced injury via mass spectrometry. *Health Phys.* **2014**, *106*, 106–19.

(24) Wang, C.; Yang, J.; Nie, J. Plasma phospholipid metabolic profiling and biomarkers of rats following radiation exposure based on liquid chromatography-mass spectrometry technique. *Biomed. Chromatogr.* **2009**, *23*, 1079–85.

(25) Tyurina, Y. Y.; Tyurin, V. A.; Kapralova, V. I.; Wasserloos, K.; Mosher, M.; Epperly, M. W.; Greenberger, J. S.; Pitt, B. R.; Kagan, V. E. Oxidative lipidomics of gamma-radiation-induced lung injury: mass spectrometric characterization of cardiolipin and phosphatidylserine peroxidation. *Radiat. Res.* **2011**, *175*, 610–21.

(26) Tyurina, Y. Y.; Tyurin, V. A.; Epperly, M. W.; Greenberger, J. S.; Kagan, V. E. Oxidative lipidomics of gamma-irradiation-induced intestinal injury. *Free Radical Biol. Med.* **2008**, *44*, 299–314.

(27) Laiakis, E. C.; Hyduke, D. R.; Fornace, A. J. Comparison of mouse urinary metabolic profiles after exposure to the inflammatory stressors gamma radiation and lipopolysaccharide. *Radiat. Res.* **2012**, *177*, 187–99.

(28) Mukherjee, D.; Coates, P. J.; Lorimore, S. A.; Wright, E. G. Responses to ionizing radiation mediated by inflammatory mechanisms. *J. Pathol.* **2014**, *232*, 289–99.

(29) Breier, M.; Wahl, S.; Prehn, C.; Fugmann, M.; Ferrari, U.; Weise, M.; Banning, F.; Seissler, J.; Grallert, H.; Adamski, J.; Lechner, A. Targeted metabolomics identifies reliable and stable metabolites in human serum and plasma samples. *PLoS One* **2014**, *9*, e89728.

(30) Mapstone, M.; Cheema, A. K.; Fiandaca, M. S.; Zhong, X.; Mhyre, T. R.; Macarthur, L. H.; Hall, W. J.; Fisher, S. G.; Peterson, D. R.; Haley, J. M.; Nazar, M. D.; Rich, S. A.; Berlau, D. J.; Peltz, C. B.; Tan, M. T.; Kawas, C. H.; Federoff, H. J. Plasma phospholipids identify antecedent memory impairment in older adults. *Nat. Med.* **2014**, *20*, 415–8.

(31) Strassburg, K.; Huijbrechts, A. M.; Kortekaas, K. A.; Lindeman, J. H.; Pedersen, T. L.; Dane, A.; Berger, R.; Brenkman, A.; Hankemeier, T.; van Duynhoven, J.; Kalkhoven, E.; Newman, J. W.; Vreeken, R. J. Quantitative profiling of oxylipins through comprehensive LC−MS/MS analysis: application in cardiac surgery. *Anal. Bioanal. Chem.* **2012**, *404*, 1413–26.

(32) Wishart, D. S.; Jewison, T.; Guo, A. C.; Wilson, M.; Knox, C.; Liu, Y.; Djoumbou, Y.; Mandal, R.; Aziat, F.; Dong, E.; Bouatra, S.; Sinelnikov, I.; Arndt, D.; Xia, J.; Liu, P.; Yallou, F.; Bjorndahl, T.; Perez-Pineiro, R.; Eisner, R.; Allen, F.; Neveu, V.; Greiner, R.; Scalbert, A. HMDB 3.0—The Human Metabolome Database in 2013. *Nucleic Acids Res.* **2013**, *41*, D801–7.

(33) Mak, T. D.; Laiakis, E. C.; Goudarzi, M.; Fornace, A. J., Jr. MetaboLyzer: a novel statistical workflow for analyzing Postprocessed LC−MS metabolomics data. *Anal. Chem.* **2014**, *86*, 506–13.

(34) Xia, J.; Mandal, R.; Sinelnikov, I. V.; Broadhurst, D.; Wishart, D. S. MetaboAnalyst 2.0—a comprehensive server for metabolomic data analysis. *Nucleic Acids Res.* **2012**, *40*, W127−33.

(35) Williams, J. P.; Brown, S. L.; Georges, G. E.; Hauer-Jensen, M.; Hill, R. P.; Huser, A. K.; Kirsch, D. G.; Macvittie, T. J.; Mason, K. A.; Medhora, M. M.; Moulder, J. E.; Okunieff, P.; Otterson, M. F.; Robbins, M. E.; Smathers, J. B.; McBride, W. H. Animal models for medical countermeasures to radiation exposure. *Radiat. Res.* **2010**, *173*, 557−78.

(36) Hall, E. J.; Giaccia, A. *Radiobiology for the Radiologist*; Lipincott William &Wilkins: Philadelphia, PA, 2011.

(37) Shadyro, O. I.; Yurkova, I. L.; Kisel, M. A.; Brede, O.; Arnhold, J. Radiation-induced fragmentation of cardiolipin in a model membrane. *Int. J. Radiat. Biol.* **2004**, *80*, 239−45.

(38) Haimovitz-Friedman, A.; Kan, C. C.; Ehleiter, D.; Persaud, R. S.; McLoughlin, M.; Fuks, Z.; Kolesnick, R. N. Ionizing radiation acts on cellular membranes to generate ceramide and initiate apoptosis. *J. Exp. Med.* **1994**, *180*, 525−35.

(39) Santana, P.; Pena, L. A.; Haimovitz-Friedman, A.; Martin, S.; Green, D.; McLoughlin, M.; Cordon-Cardo, C.; Schuchman, E. H.; Fuks, Z.; Kolesnick, R. Acid sphingomyelinase-deficient human lymphoblasts and mice are defective in radiation-induced apoptosis. *Cell* **1996**, *86*, 189−99.

(40) Engelmann, B.; Brautigam, C.; Thiery, J. Plasmalogen phospholipids as potential protectors against lipid peroxidation of low density lipoproteins. *Biochem. Biophys. Res. Commun.* **1994**, *204*, 1235−42.

(41) Han, X. L.; Gross, R. W. Plasmenylcholine and phosphatidylcholine membrane bilayers possess distinct conformational motifs. *Biochemistry* **1990**, *29*, 4992−6.

(42) Morandat, S.; Bortolato, M.; Anker, G.; Doutheau, A.; Lagarde, M.; Chauvet, J. P.; Roux, B. Plasmalogens protect unsaturated lipids against UV-induced oxidation in monolayer. *Biochim. Biophys. Acta* **2003**, *1616*, 137−46.

(43) Brosche, T.; Platt, D. The biological significance of plasmalogens in defense against oxidative damage. *Exp. Gerontol.* **1998**, *33*, 363−9.

(44) Lessig, J.; Fuchs, B. Plasmalogens in biological systems: their role in oxidative processes in biological membranes, their contribution to pathological processes and aging and plasmalogen analysis. *Curr. Med. Chem.* **2009**, *16*, 2021−41.

(45) Engelmann, B. Plasmalogens: targets for oxidants and major lipophilic antioxidants. *Biochem. Soc. Trans.* **2004**, *32*, 147−50.

(46) Stadelmann-Ingrand, S.; Pontcharraud, R.; Fauconneau, B. Evidence for the reactivity of fatty aldehydes released from oxidized plasmalogens with phosphatidylethanolamine to form Schiff base adducts in rat brain homogenates. *Chem. Phys. Lipids* **2004**, *131*, 93−105.

(47) Braverman, N. E.; Moser, A. B. Functions of plasmalogen lipids in health and disease. *Biochim. Biophys. Acta* **2012**, *1822*, 1442−52.

(48) Dalli, J.; Colas, R. A.; Serhan, C. N. Novel n-3 immunoresolvents: structures and actions. *Sci. Rep.* **2013**, *3*, 1940.

(49) Serhan, C. N. Systems approach with inflammatory exudates uncovers novel anti-inflammatory and pro-resolving mediators. *Prostaglandins, Leukotrienes Essent. Fatty Acids* **2008**, *79*, 157−63.

(50) Serhan, C. N.; Samuelsson, B. Lipoxins: a new series of eicosanoids (biosynthesis, stereochemistry, and biological activities). *Adv. Exp. Med. Biol.* **1988**, *229*, 1−14.

(51) Bazan, N. G.; Calandria, J. M.; Gordon, W. C. Docosahexaenoic acid and its derivative neuroprotectin D1 display neuroprotective properties in the retina, brain and central nervous system. *Nestle Nutr. Inst. Workshop Ser.* **2013**, *77*, 121−31.

(52) Nicolaou, A.; Masoodi, M.; Mir, A. Lipidomic analysis of prostanoids by liquid chromatography−electrospray tandem mass spectrometry. *Methods Mol. Biol.* **2009**, *579*, 271−86.

(53) Yang, H. J.; Youn, H.; Seong, K. M.; Yun, Y. J.; Kim, W.; Kim, Y. H.; Lee, J. Y.; Kim, C. S.; Jin, Y. W.; Youn, B. Psoralidin, a dual inhibitor of COX-2 and 5-LOX, regulates ionizing radiation (IR)-induced pulmonary inflammation. *Biochem. Pharmacol.* **2011**, *82*, 524−34.

(54) Milas, L.; Kishi, K.; Hunter, N.; Mason, K.; Masferrer, J. L.; Tofilon, P. J. Enhancement of tumor response to gamma-radiation by an inhibitor of cyclooxygenase-2 enzyme. *J. Natl. Cancer Inst.* **1999**, *91*, 1501−4.

(55) Zhou, H.; Ivanov, V. N.; Gillespie, J.; Geard, C. R.; Amundson, S. A.; Brenner, D. J.; Yu, Z.; Lieberman, H. B.; Hei, T. K. Mechanism of radiation-induced bystander effect: role of the cyclooxygenase-2 signaling pathway. *Proc. Natl. Acad. Sci. U.S.A.* **2005**, *102*, 14641−6.

(56) Lorimore, S. A.; Coates, P. J.; Scobie, G. E.; Milne, G.; Wright, E. G. Inflammatory-type responses after exposure to ionizing radiation in vivo: a mechanism for radiation-induced bystander effects? *Oncogene* **2001**, *20*, 7085−95.

(57) Morgan, W. F.; Sowa, M. B. Non-targeted effects induced by ionizing radiation: mechanisms and potential impact on radiation induced health effects. *Cancer Lett.* **2013**, 10.1016/j.canlet.2013.09.009.

(58) Hayashi, T.; Morishita, Y.; Khattree, R.; Misumi, M.; Sasaki, K.; Hayashi, I.; Yoshida, K.; Kajimura, J.; Kyoizumi, S.; Imai, K.; Kusunoki, Y.; Nakachi, K. Evaluation of systemic markers of inflammation in atomic-bomb survivors with special reference to radiation and age effects. *FASEB J.* **2012**, *26*, 4765−73.

(59) Hayashi, T.; Morishita, Y.; Kubo, Y.; Kusunoki, Y.; Hayashi, I.; Kasagi, F.; Hakoda, M.; Kyoizumi, S.; Nakachi, K. Long-term effects of radiation dose on inflammatory markers in atomic bomb survivors. *Am. J. Med.* **2005**, *118*, 83−6.

(60) Tominaga, H.; Kodama, S.; Matsuda, N.; Suzuki, K.; Watanabe, M. Involvement of reactive oxygen species (ROS) in the induction of genetic instability by radiation. *J. Radiat. Res.* **2004**, *45*, 181−8.

(61) Sobolewski, C.; Cerella, C.; Dicato, M.; Ghibelli, L.; Diederich, M. The role of cyclooxygenase-2 in cell proliferation and cell death in human malignancies. *Int. J. Cell Biol.* **2010**, *2010*, 215158.

(62) Wang, M. T.; Honn, K. V.; Nie, D. Cyclooxygenases, prostanoids, and tumor progression. *Cancer Metastasis Rev.* **2007**, *26*, 525−34.

(63) Yan, M.; Myung, S. J.; Fink, S. P.; Lawrence, E.; Lutterbaugh, J.; Yang, P.; Zhou, X.; Liu, D.; Rerko, R. M.; Willis, J.; Dawson, D.; Tai, H. H.; Barnholtz-Sloan, J. S.; Newman, R. A.; Bertagnolli, M. M.; Markowitz, S. D. 15-Hydroxyprostaglandin dehydrogenase inactivation as a mechanism of resistance to celecoxib chemoprevention of colon tumors. *Proc. Natl. Acad. Sci. U.S.A.* **2009**, *106*, 9409−13.

(64) Bruins, M. J.; Dane, A. D.; Strassburg, K.; Vreeken, R. J.; Newman, J. W.; Salem, N., Jr.; Tyburczy, C.; Brenna, J. T. Plasma oxylipin profiling identifies polyunsaturated vicinal diols as responsive to arachidonic acid and docosahexaenoic acid intake in growing piglets. *J. Lipid Res.* **2013**, *54*, 1598−607.

(65) Morisseau, C.; Hammock, B. D. Impact of soluble epoxide hydrolase and epoxyeicosanoids on human health. *Annu. Rev. Pharmacol. Toxicol.* **2013**, *53*, 37−58.

(66) Capdevila, J. H.; Falck, J. R. Biochemical and molecular properties of the cytochrome P450 arachidonic acid monooxygenases. *Prostaglandins Other Lipid Mediators* **2002**, *68−69*, 325−44.

(67) Spector, A. A. Arachidonic acid cytochrome P450 epoxygenase pathway. *J. Lipid Res.* **2009**, *50*, S52−6.

(68) Zeldin, D. C. Epoxygenase pathways of arachidonic acid metabolism. *J. Biol. Chem.* **2001**, *276*, 36059−62.

(69) Morin, C.; Sirois, M.; Echave, V.; Albadine, R.; Rousseau, E. 17,18-Epoxyeicosatetraenoic acid targets PPARgamma and p38 mitogen-activated protein kinase to mediate its anti-inflammatory effects in the lung: role of soluble epoxide hydrolase. *Am. J. Respir. Cell Mol. Biol.* **2010**, *43*, 564−75.

(70) Morisseau, C.; Inceoglu, B.; Schmelzer, K.; Tsai, H. J.; Jinks, S. L.; Hegedus, C. M.; Hammock, B. D. Naturally occurring monoepoxides of eicosapentaenoic acid and docosahexaenoic acid are bioactive antihyperalgesic lipids. *J. Lipid Res.* **2010**, *51*, 3481−90.

(71) VanRollins, M. Epoxygenase metabolites of docosahexaenoic and eicosapentaenoic acids inhibit platelet aggregation at concentrations below those affecting thromboxane synthesis. *J. Pharmacol. Exp. Ther.* **1995**, *274*, 798−804.

(72) Morin, C.; Sirois, M.; Echave, V.; Rizcallah, E.; Rousseau, E. Relaxing effects of 17(18)-EpETE on arterial and airway smooth muscles in human lung. *Am. J. Physiol.: Lung Cell Mol. Physiol.* **2009**, *296*, L130−9.

(73) Shearer, G. C.; Harris, W. S.; Pedersen, T. L.; Newman, J. W. Detection of omega-3 oxylipins in human plasma and response to treatment with omega-3 acid ethyl esters. *J. Lipid Res.* **2010**, *51*, 2074−81.

(74) Newman, J. W.; Stok, J. E.; Vidal, J. D.; Corbin, C. J.; Huang, Q.; Hammock, B. D.; Conley, A. J. Cytochrome p450-dependent lipid metabolism in preovulatory follicles. *Endocrinology* **2004**, *145*, 5097−105.

(75) Keenan, A. H.; Pedersen, T. L.; Fillaus, K.; Larson, M. K.; Shearer, G. C.; Newman, J. W. Basal omega-3 fatty acid status affects fatty acid and oxylipin responses to high-dose n3-HUFA in healthy volunteers. *J. Lipid Res.* **2012**, *53*, 1662−9.

(76) Nording, M. L.; Yang, J.; Georgi, K.; Hegedus Karbowski, C.; German, J. B.; Weiss, R. H.; Hogg, R. J.; Trygg, J.; Hammock, B. D.; Zivkovic, A. M. Individual variation in lipidomic profiles of healthy subjects in response to omega-3 fatty acids. *PLoS One* **2013**, *8*, e76575.

(77) Arnold, C.; Markovic, M.; Blossey, K.; Wallukat, G.; Fischer, R.; Dechend, R.; Konkel, A.; von Schacky, C.; Luft, F. C.; Muller, D. N.; Rothe, M.; Schunck, W. H. Arachidonic acid-metabolizing cytochrome P450 enzymes are targets of {omega}-3 fatty acids. *J. Biol. Chem.* **2010**, *285*, 32720−33.

(78) Astarita, G.; McKenzie, J. H.; Wang, B.; Strassburg, K.; Doneanu, A.; Johnson, J.; Baker, A.; Hankemeier, T.; Murphy, J.; Vreeken, R. J.; Langridge, J.; Kang, J. X. A protective lipidomic biosignature associated with a balanced omega-6/omega-3 ratio in fat-1 transgenic mice. *PLoS One* **2014**, *9*, e96221.

(79) Shan, Y. X.; Jin, S. Z.; Liu, X. D.; Liu, Y.; Liu, S. Z. Ionizing radiation stimulates secretion of pro-inflammatory cytokines: dose-response relationship, mechanisms and implications. *Radiat. Environ. Biophys.* **2007**, *46*, 21−9.

(80) Schaue, D.; Kachikwu, E. L.; McBride, W. H. Cytokines in radiobiological responses: a review. *Radiat. Res.* **2012**, *178*, 505−23.

(81) Serhan, C. N.; Hong, S.; Gronert, K.; Colgan, S. P.; Devchand, P. R.; Mirick, G.; Moussignac, R. L. Resolvins: a family of bioactive products of omega-3 fatty acid transformation circuits initiated by aspirin treatment that counter proinflammation signals. *J. Exp. Med.* **2002**, *196*, 1025−37.

(82) Colas, R. A.; Shinohara, M.; Dalli, J.; Chiang, N.; Serhan, C. N. Identification and signature profiles for pro-resolving and inflammatory lipid mediators in human tissue. *Am. J. Physiol.: Cell Physiol.* **2014**, *307*, C39−C54.

(83) Lee, J. C.; Krochak, R.; Blouin, A.; Kanterakis, S.; Chatterjee, S.; Arguiri, E.; Vachani, A.; Solomides, C. C.; Cengel, K. A.; Christofidou-Solomidou, M. Dietary flaxseed prevents radiation-induced oxidative lung damage, inflammation and fibrosis in a mouse model of thoracic radiation injury. *Cancer Biol. Ther.* **2009**, *8*, 47−53.

(84) Christofidou-Solomidou, M.; Tyagi, S.; Tan, K. S.; Hagan, S.; Pietrofesa, R.; Dukes, F.; Arguiri, E.; Heitjan, D. F.; Solomides, C. C.; Cengel, K. A. Dietary flaxseed administered post thoracic radiation treatment improves survival and mitigates radiation-induced pneumonopathy in mice. *BMC Cancer* **2011**, *11*, 269.

(85) Zhang, Y.; Zhou, X.; Li, C.; Wu, J.; Kuo, J. E.; Wang, C. Assessment of early triage for acute radiation injury in rat model based on urinary amino acid target analysis. *Mol. BioSyst.* **2014**, *10*, 1441−9.

(86) Lutgens, L. C.; Deutz, N.; Granzier-Peeters, M.; Beets-Tan, R.; De Ruysscher, D.; Gueulette, J.; Cleutjens, J.; Berger, M.; Wouters, B.; von Meyenfeldt, M.; Lambin, P. Plasma citrulline concentration: a surrogate end point for radiation-induced mucosal atrophy of the small bowel. A feasibility study in 23 patients. *Int. J. Radiat. Oncol., Biol., Phys.* **2004**, *60*, 275−85.

(87) Onal, C.; Kotek, A.; Unal, B.; Arslan, G.; Yavuz, A.; Topkan, E.; Yavuz, M. Plasma citrulline levels predict intestinal toxicity in patients treated with pelvic radiotherapy. *Acta Oncol.* **2011**, *50*, 1167−74.

(88) Rieger, K. E.; Hong, W. J.; Tusher, V. G.; Tang, J.; Tibshirani, R.; Chu, G. Toxicity from radiation therapy associated with abnormal transcriptional responses to DNA damage. *Proc. Natl. Acad. Sci. U.S.A.* **2004**, *101*, 6635−40.

(89) Popanda, O.; Ebbeler, R.; Twardella, D.; Helmbold, I.; Gotzes, F.; Schmezer, P.; Thielmann, H. W.; von Fournier, D.; Haase, W.; Sautter-Bihl, M. L.; Wenz, F.; Bartsch, H.; Chang-Claude, J. Radiation-induced DNA damage and repair in lymphocytes from breast cancer patients and their correlation with acute skin reactions to radiotherapy. *Int. J. Radiat. Oncol., Biol., Phys.* **2003**, *55*, 1216−25.

(90) Crompton, N. E.; Miralbell, R.; Rutz, H. P.; Ersoy, F.; Sanal, O.; Wellmann, D.; Bieri, S.; Coucke, P. A.; Emery, G. C.; Shi, Y. Q.; Blattmann, H.; Ozsahin, M. Altered apoptotic profiles in irradiated patients with increased toxicity. *Int. J. Radiat. Oncol., Biol., Phys.* **1999**, *45*, 707−14.

(91) Barber, J. B.; Burrill, W.; Spreadborough, A. R.; Levine, E.; Warren, C.; Kiltie, A. E.; Roberts, S. A.; Scott, D. Relationship between in vitro chromosomal radiosensitivity of peripheral blood lymphocytes and the expression of normal tissue damage following radiotherapy for breast cancer. *Radiother. Oncol.* **2000**, *55*, 179−86.

(92) Skiold, S.; Naslund, I.; Brehwens, K.; Andersson, A.; Wersall, P.; Lidbrink, E.; Harms-Ringdahl, M.; Wojcik, A.; Haghdoost, S. Radiation-induced stress response in peripheral blood of breast cancer patients differs between patients with severe acute skin reactions and patients with no side effects to radiotherapy. *Mutat. Res.* **2013**, *756*, 152−7.

(93) Haghdoost, S.; Svoboda, P.; Naslund, I.; Harms-Ringdahl, M.; Tilikides, A.; Skog, S. Can 8-oxo-dG be used as a predictor for individual radiosensitivity? *Int. J. Radiat. Oncol., Biol., Phys.* **2001**, *50*, 405−10.